

# Multiple bound states in scissor-shaped waveguides

Evgeny N. Bulgakov<sup>a</sup>, Pavel Exner<sup>b,c</sup>, Konstantin N. Pichugin,<sup>a</sup>  
and Almas F. Sadreev<sup>a,d</sup>

<sup>a</sup> Institute of Physics, 660036 Krasnoyarsk, Russia

<sup>b</sup> Nuclear Physics Institute, Czech Academy of Sciences, 25068 Řež

<sup>c</sup> Doppler Institute, Czech Technical University, Břehová 7,  
11519 Prague, Czechia

<sup>d</sup> Department of Physics and Measurement Technology,  
Linköping University, 581 83 Linköping, Sweden

We study bound states of the two-dimensional Helmholtz equations with Dirichlet boundary conditions in an open geometry given by two straight leads of the same width which cross at an angle  $\theta$ . Such a four-terminal junction with a tunable  $\theta$  can be realized experimentally if a right-angle structure is filled by a ferrite. It is known that for  $\theta = 90^\circ$  there is one proper bound state and one eigenvalue embedded in the continuum. We show that the number of eigenvalues becomes larger with increasing asymmetry and the bound-state energies are increasing as functions of  $\theta$  in the interval  $(0, 90^\circ)$ . Moreover, states which are sufficiently strongly bent exist in pairs with a small energy difference and opposite parities. Finally, we discuss how with increasing  $\theta$  the bound states transform into the quasi-bound states with a complex wave vector.

PACS numbers: 42.25.Bs, 03.65.Ge, 73.40.Lq, 03.75.Be

## I. INTRODUCTION

The question of a possible existence of modes trapped in open two-dimensional systems has been a classic in the theory of waveguides; trapped modes due to particular boundary conditions were studied already half a century ago [1]. However, only much later it was realized that the introduction of bends and crossings into waveguides gives rise generally to confined states, or bound states which exist below the cutoff frequency for the waveguide [2, 3, 4, 5, 6, 7, 8, 9, 10, 11, 12, 13, 14, 15, 16]. The existence of such states has both theoretical significance and implications for possible applications. They have been subsequently discussed in many papers, in addition to those mentioned above we refer to the monograph [17] and the bibliography there.

In this paper we consider a system of two straight waveguides of the same width  $d$  which cross at a nonzero angle  $\theta$ . The right-angle case was one of the first examples where the binding was studied. Schult, Ravenhall, and Wyld [7] showed the existence of two bound states. One of them is a true bound state at the energy  $0.66(\pi/d)^2$  in the natural units, while the other one at  $3.72(\pi/d)^2$  is embedded into the continuum and does not decay due to the symmetry. The latter corresponds to the single bound state in an L-shaped tube of width  $d/2$  [5]. Our aim is to show how the spectrum of such a junction, which we will call for the sake of brevity “scissors” in the following, changes as the angle  $\theta$  varies over the interval  $(0, 90^\circ)$ .

We will show that as we go further from the cross symmetry if the right-angle structure, new bound states emerge from the continuum. In strongly skewed junction corresponding to a small  $\theta$  there are many of them. The mechanism responsible for their existence is the same as

for the bound states in sharply broken tubes studied theoretically and experimentally in [10, 12], namely a long part of the junction where there is a transverse contribution to the energy is substantially lower than  $(\pi/d)^2$ . In the present case, however, the system has a mirror symmetry with respect to the axis of the complement angle  $180^\circ - \theta$  and the bound states exist in pairs corresponding to different parity. We will show that as the angle  $\theta$  diminishes and the states become strongly bound, the energy gap between the even and odd member of the pair vanishes exponentially fast. We also study the behavior around the critical values  $\theta_c$  where the bound states emerge from the continuum. Our numerical analysis shows that the binding energy of the weakly-coupled states behaves as correction  $\approx \pi^2 - \gamma(\theta_c - \theta)^2$

## II. FERRITE FILLED MICROWAVE WAVEGUIDES AS A WAY TO VARY THE ANGLE OF THE SCISSORS

Before analyzing the scissor spectrum, let us discuss how such a structure can be realized experimentally as a microwave device. It is no problem, of course, to build crossed waveguides in the ways explained in [17]. However, in such a setting it is not easy to vary the geometry continuously. Our point here is that this goal can be achieved with a structure of a fixed angle if the latter is filled by a ferrite with an axial magnetic anisotropy and an external magnetic field is applied. We will show that this leads to an effective angle controlled by the field strength, following the idea which was first applied to the equivalence between a ferrite-filled squared resonator with an external magnetic field and a field-free rhombic polygon [18].

To explain the mechanism of this equivalence we begin with the Maxwell equations which in the presence of a material have the form

$$\begin{aligned}\nabla \cdot \mathbf{E} &= \nabla \cdot \mathbf{B} = 0, \\ \nabla \times \mathbf{E} &= -ik\mathbf{B}, \quad \nabla \times \mathbf{H} = ik\mathbf{E}, \\ \mathbf{B} &= \hat{\mu}\mathbf{H},\end{aligned}\quad (1)$$

where  $\mathbf{E}$  is the electric field,  $\mathbf{H}$  is the magnetic field,  $\mathbf{B}$  is the magnetic induction,  $k = \omega/c$  and  $\omega$  is an eigen-frequency with the wave vector  $k$ . We suppose that the material has a magnetic anisotropy corresponding to an anisotropic permeability  $\hat{\mu} = 1 + 4\pi\hat{\chi}$  with [19]

$$\hat{\chi} = \begin{pmatrix} \chi_{xx} & \chi_{xy} & 0 \\ \chi_{xy} & \chi_{yy} & 0 \\ 0 & 0 & 0 \end{pmatrix}, \quad (2)$$

where

$$\chi_{xx} = \frac{g\Omega_1 M_0}{\Omega_1 \Omega_2 - \omega^2}, \quad \chi_{yy} = \frac{g\Omega_2 M_0}{\Omega_1 \Omega_2 - \omega^2}$$

and Eq(3)

$$\chi_{xy} = -\chi_{yx} = \frac{i\omega g\Omega_1 M_0}{\Omega_1 \Omega_2 - \omega^2}. \quad (3)$$

Here  $g$  is the magnetomechanical factor,  $M_0$  is the magnetization of the material,

$$\begin{aligned}\Omega_1 &= gM_0 \left( \frac{\mathbf{M}_0 \mathbf{H}_0^{(i)}}{M_0^2} + \frac{gK_a}{M_0} \cos^2 \Psi \right), \\ \Omega_2 &= gM_0 \left( \frac{\mathbf{M}_0 \mathbf{H}_0^{(i)}}{M_0^2} + \frac{gK_a}{M_0} \cos 2\Psi \right)\end{aligned}\quad (4)$$

and  $K_a$  characterizes the anisotropy type: it is an easy plane anisotropy for  $K_a > 0$  and an easy axis anisotropy for  $K_a < 0$ . In what follows we suppose that the material has an easy plane magnetic anisotropy,  $K_a > 0$ , in which case the intrinsic magnetic field is equal to

$$\mathbf{H} = \mathbf{H}_0 - 4\pi M_{0z} \mathbf{e}_z.$$

On the relations (4)  $\Psi$  is the angle between the anisotropy axis  $\mathbf{N}$  and the magnetization  $\mathbf{M}_0$ . We choose the latter to coincide with the  $z$  axis along the magnetization, while the  $x$  axis lies in the plane spanned by the vectors  $\mathbf{N}$  and  $\mathbf{M}_0$ .

In the simplest case of an easy plane magnetic material we have  $\mathbf{M}_0 \perp \mathbf{N}$  and  $\mathbf{M}_0 \parallel \mathbf{H}_0^{(i)}$  with  $\Psi = \pi/2$ , so we obtain from (4)

$$\begin{aligned}\Omega_1 &= g(H_0 - 4\pi M_0), \\ \Omega_2 &= g(H_0 - 4\pi M_0) + gK_a M_0.\end{aligned}\quad (5)$$

This is shown in Fig. 1 where the  $z$  axis is perpendicular to the plane of the waveguide. We seek a two-dimensional solution of the Maxwell equations (1) shown at this figure

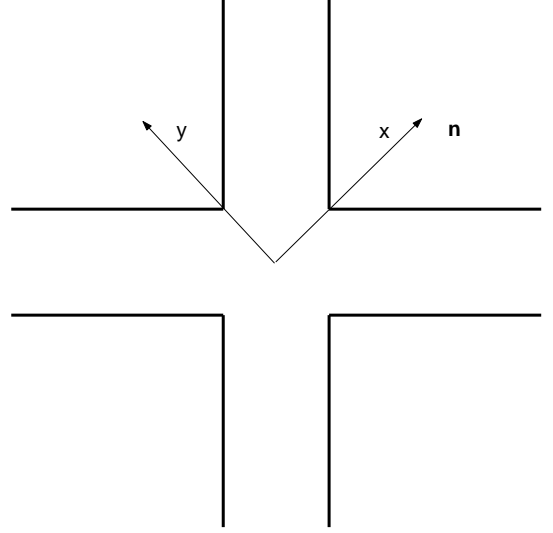


FIG. 1: Schematic view of the cross-bar resonator (scissors with  $\theta = 90^\circ$ ) filled with ferrite where  $\mathbf{M}$  is the magnetization of ferrite and  $\mathbf{N}$  is the anisotropy field.

in the form  $\mathbf{E}(x, y) = E(x, y)\mathbf{e}_z$ . The fields  $\mathbf{B}, \mathbf{H}$  lay in the plane  $x, y$  and depend on  $x, y$  too. Then the first equation is satisfied, while the third one gives

$$-ikB_x = \frac{\partial E_z}{\partial y}, \quad -ikB_y = -\frac{\partial E_z}{\partial x}, \quad (6)$$

and finally, the fourth Maxwell equation can be rewritten as

$$ikE_z = \frac{\partial H_y}{\partial x} - \frac{\partial H_x}{\partial y}. \quad (7)$$

Using the explicit form of the permeability given by (2) we get

$$\mathbf{B} = \begin{pmatrix} \mu_{xx} & \mu_{xy} & 0 \\ \mu_{yx} & \mu_{yy} & 0 \\ 0 & 0 & 1 \end{pmatrix} \begin{pmatrix} H_x \\ H_y \\ H_z \end{pmatrix}.$$

Combining this with Eq. (6) we obtain

$$\begin{pmatrix} H_x \\ H_y \end{pmatrix} = \frac{1}{D} \begin{pmatrix} \mu_{yy} & \mu_{xy} \\ \mu_{yx} & \mu_{xx} \end{pmatrix} \begin{pmatrix} \frac{i}{k} \frac{\partial E_z}{\partial y} \\ -\frac{i}{k} \frac{\partial E_z}{\partial x} \end{pmatrix}, \quad (8)$$

where we have denoted

$$D = \mu_{xx}\mu_{yy} - \mu_{xy}\mu_{yx}.$$

Substituting Eq. (8) into Eq. (7) we obtain

$$\mu_{xx} \frac{\partial^2 E_z}{\partial x^2} + \mu_{yy} \frac{\partial^2 E_z}{\partial y^2} + (\mu_{xy} + \mu_{yx}) \frac{\partial^2 E_z}{\partial x \partial y} + Dk^2 E_z = 0. \quad (9)$$

The key observation is that the mixed derivatives in the last equation can be eliminated by the coordinate transformation

$$\begin{pmatrix} x' \\ y' \end{pmatrix} = \begin{pmatrix} -\frac{\sqrt{\mu_{xx}\mu_{yy} - (\mu_{xy} + \mu_{yx})^2/4}}{2\mu_{xx}} & 0 \\ -\frac{\mu_{xy} + \mu_{yx}}{2\mu_{xx}} & 1 \end{pmatrix} \begin{pmatrix} x \\ y \end{pmatrix} \quad (10)$$

which allows us to cast Eq. (9) into the following simple form

$$\nabla^2 E_z + \lambda k^2 E_z = 0, \quad (11)$$

where

$$\lambda = \sqrt{\frac{\mu_{yy}}{\mu_{xx}}}; \quad (12)$$

we have taken into account that  $\mu_{xy} + \mu_{yx} = 0$  holds in accordance with (3).

The transformation (10) defines a relation between a right-angle cross structure and a skewed one with an angle defined by  $\lambda$ . It is too daring, however, to speak about a full equivalence, because it is clear from the formulas expressing the elements of (2) that the angle depends on the eigenfrequencies involved. Let us ask under which conditions this dependence of the geometrical factor (12) can be suppressed. Substituting into (12) the expressions (5) we get

$$\lambda^2 = \frac{\Omega_1 \Omega_2 - \omega^2 + 4\pi g \Omega_2 M_0}{\Omega_1 \Omega_2 - \omega^2 + 4\pi g \Omega_1 M_0}. \quad (13)$$

Following to [18] we can simplify this expression if to assume that

$$gK_a/M_0 \gg \max\{gH_0, 4\pi g M_0, \omega\}. \quad (14)$$

For typical ferrites  $K_a \sim 10^6$  erg/cm<sup>3</sup> and  $4\pi M_0 \sim 100$  Oe [19]. Taking the magnetomechanical factor  $g \sim 10^7$  sec<sup>-1</sup> Oe<sup>-1</sup> we obtain from (14)  $H_0 \ll 10^4$  Oe,  $\omega \ll 10^{11}$  what would require very wide waveguides of a width  $d \sim 10$  cm. However, there are ferrites with  $K_a \sim 10^8$  erg/cm<sup>3</sup> which lead to the inequality  $\omega \ll 10^{13}$ . Hence in this case we are able to use standard waveguides the width of which is of order 1 cm. Then we can simplify the geometrical factor of the waveguide to the form

$$\lambda^2 = \frac{H_0}{H_0 - 4\pi M_0}. \quad (15)$$

This formula gives a remarkable possibility to change the angle of the scissors

$$\theta = 2 \arctan \lambda \quad (16)$$

by means of an external magnetic field applied along the magnetization direction.

Moreover if to apply strong magnetic field  $gH_0 \gg \omega$  or  $H_0 \gg 10^4$  Oe, then it follows from formula (13) that

$$\lambda^2 = \frac{H_0}{H_0 + gK_a/M_0}. \quad (17)$$

On this case also the effective angle of the structure can be tuned by variation of the external magnetic field.

### III. BOUND STATES AND RESONANCES

First we review some general properties of the bound states which can be derived by the standard methods of dealing with Laplace operator with Dirichlet boundary conditions, the Dirichlet-Neumann bracketing [20] and eigenvalue variation with respect to the change of the domain [21]. The problem has two mirror symmetries with respect to the axis of the angle  $\theta$  which we call scissor axis, and with respect to the axis of the larger angle  $180^\circ - \theta$  which we call the second axis. Using the mentioned methods together with an eigenvalue-in-the-box estimate analogous to that employed in [10] we find that

- (i) every bound state is even w.r.t. the scissor axis,
- (ii) with respect to the second axis the bound states can have both parities which are alternating if the bound states are arranged according to their energies,
- (iii) as  $\theta$  becomes smaller new bound states emerge from the continuum. The number  $N$  of bound states satisfies the inequality  $N \geq 2c\pi^{-1}(90^\circ/\theta)$  with  $c = (1 - 2^{-2/3})^{3/2} \approx 0.225$ . While it is not good around  $\theta = 90^\circ$ , where we know that  $N = 1$  from [7], it is asymptotically exact as  $\theta \rightarrow 0$ ,
- (iv) all the bound-state energies are monotonously increasing functions of  $\theta$ .

The angle dependence of the bound-state energies has different regimes. In the weak-coupling regime when the scissors are closing and just passed the critical angle  $\theta_c$  at which a new bound state appeared, our numerical analysis shows that the binding energy of the weakly-coupled states behaves as  $\approx \pi^2 - \gamma(\theta_c - \theta)^2$  with some constant  $\gamma$  which depends on the particular state. On the other hand, strongly bound states corresponding to a small  $\theta$  are in the leading order determined by the one dimensional potential well given by the lowest transverse eigenvalue [22]. The second axis determining the parity of the solution is then deep in the classically forbidden region, so we can conclude that

- (v) as  $\theta$  becomes smaller the bound states group into pairs with opposite parities and the energy gap between them is exponentially small as  $\theta \rightarrow 0$ .

After these general results let us pass to the numerical solution. We use three different methods. The most common among them is the boundary integral method [23]. In combination with the above general results, it provides a rather complete information about the discrete spectrum.

On the other hand, the boundary integral method tells us nothing about the scattering problem in the scissor structure. We are interested in particular in the scattering resonances associated with quasibound states, which are characterized of complex values of energy at which the analytically continued resolvent has a pole singularity. A suitable method to treat this problem is the exterior complex scaling. The method was suggested in the

seminal paper [24] and has developed into an efficient computational tool – see [25] and reference therein. The use of exterior complex scaling for waveguide structures was first proposed in [26], here we employ it in the form presented in [27]. Before the proper scaling we pass to right-angle scissors by means of the coordinate change

$$\begin{cases} x' = x \sin \alpha - y \cos \alpha \\ y' = y \end{cases} \quad (18)$$

which takes the Hamiltonian to a unitarily equivalent operator acting as

$$\hat{H}\Psi = \left( -\frac{\partial^2}{\partial x'^2} - \frac{\partial^2}{\partial y'^2} + 2 \cos \alpha \frac{\partial^2}{\partial x' \partial y'} \right) \Psi \quad (19)$$

Now we apply the scaling transformation to the longitudinal variable in the structure arms which leaves the central area unchanged,  $x = g(X)$  and  $y = g(Y)$ , which yields the scaled Hamiltonian

$$\hat{H} = -\nabla \left[ \begin{pmatrix} c_{11}(X, Y) & c_{12}(X, Y) \\ c_{21}(X, Y) & c_{22}(X, Y) \end{pmatrix} \nabla \right] + U(X, Y) \quad (20)$$

with

$$\begin{aligned} c_{11}(X, Y) &= \frac{1}{g'^2(X)}, & c_{12}(X, Y) &= -\frac{\cos \alpha}{g'(X)g'(Y)}, \\ c_{21}(X, Y) &= -\frac{\cos \alpha}{g'(X)g'(Y)}, & c_{22}(X, Y) &= \frac{1}{g'^2(Y)}, \end{aligned}$$

and

$$\begin{aligned} U(X, Y) &= \frac{2g'(X)g'''(X) - 5g''^2(X)}{4g'(X)^4} \\ &+ \frac{2g'(Y)g'''(Y) - 5g''^2(Y)}{4g'(Y)^4} + \frac{g''(X)g''(Y)}{4g'^2(X)g'^2(Y)} 2 \cos \alpha \end{aligned}$$

The function  $g(x)$  can be chosen, e.g., as

$$g(x) = \begin{cases} x & \text{if } |x| \leq x_0 \\ \theta f(x) & \text{if } |x| > x_0 \end{cases}$$

with  $x_0$  larger than the channel halfwidth and the interpolating function  $f(x)$  such that  $f(x) = x$  for  $|x| > 2x_0$ , the function  $g(x)$  is three times differentiable and the inverse map  $g^{-1}$  exists. As long as the parameter  $\theta$  is real, the above transformation is a simple coordinate change which does not change the spectrum. However, if  $\theta$  assumes complex values we observe a different behavior in the discrete and continuous part typical in such situations [20]: each branch of the continuous spectrum of the operator (20) is rotated into the complex plane giving

$$\bigcup_{n=1}^{\infty} \{(n\pi)^2 + \theta^{-2}(0, \infty)\}$$

for  $d = 1$ . If  $\Im \theta > 0$  the rotated branches point to the lower half plane and reveal parts of other sheets of the

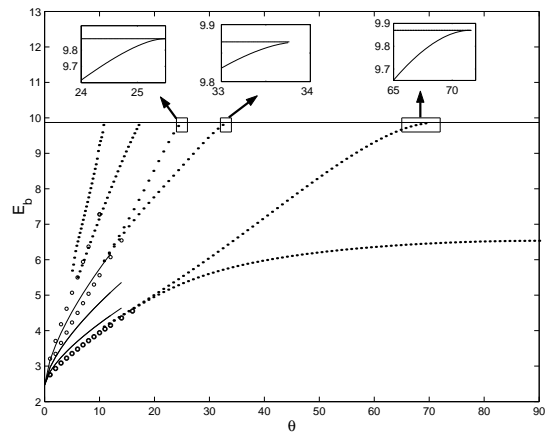


FIG. 2: Bound state energies for scissors structure as a function of the interior angle  $\theta$ . The complex scaling method data are shown by points. The boundary integral method data are shown by circles. The asymptotic formulas (22) with corresponding quantum numbers  $m = 1, 2, 3$  are given by thin solid lines. Insets above show blow up of asymptotic behavior of the bound state energies in the vicinity of bottom of propagation band  $pi^2$ .

Riemann surface of energy and we are able to see the resonance poles as complex eigenvalues of the transformed operator; the corresponding eigenfunctions are after the transformation decaying at large distances, instead of the original growing oscillations typical for Gamow functions.

Finally, the third method is based on application of infinitesimally small time-periodic perturbation. The bound states with energies below the propagation subband ( $E_b < E_0 = \pi^2$ ) do not participate in stationary transmission. However, it is possible to mix the bound state  $|b\rangle$  with propagating state  $|k\rangle$  via a time-periodic perturbation

$$V(t) = V_0 \cos(\omega t) \quad (21)$$

provided that the matrix elements of the perturbation  $\langle b|V|k\rangle \neq 0$ . Such a possibility was demonstrated for the four-terminal's Hall junction for electron transmission effected by a radiation field [15, 28]. Later the mixing of bound states with propagating modes was also realized in microwave transmission [16]. Here we similar to [29] use the time-periodic perturbation (21) as a probing one to find the bound state energy by resonant features in the transmission probability.

#### IV. NUMERICAL RESULTS

Let us show the results of numerical analysis based on the methods described above. First we plot the bound state energies as a function of the scissor angle  $\theta$ . The results of complex scale method are presented in Fig. 2 by points.

The results of boundary integral method are shown in Fig. 2 by circles. For the limit  $\theta \rightarrow 0$  the energies of

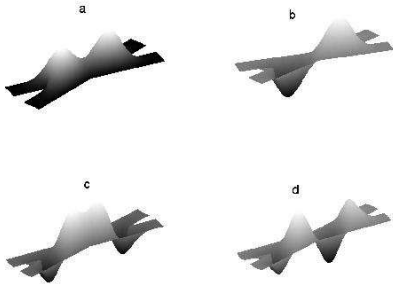


FIG. 3: The even-even and odd-even bound states for scissors structure for  $\theta = 30^\circ$ .

bound states are derived in [13] and have the following form Eq(22)

$$E_{nm} \rightarrow \frac{\pi^2}{4} [n^2 + (2n^2 + m^2/4)\theta^{2/3} + \dots] \quad (22)$$

where the quantum numbers  $n, m = 1, 2, 3, \dots$ . The factor  $1/4$  in (22) takes into account that the length of an inscribed rectangle has a length twice more than in the case of bent waveguide studied in [12, 13]. Insets above the figure show blow up of asymptotic behavior of the energies in the vicinity of the edge energy band  $E_0 = \pi^2$ . For all energies of bound states the asymptotics are  $\pi^2 - \gamma(\theta_c - \theta)^2$  where  $\gamma$  is a constant.

As it was discussed in the Introduction as the angle  $\theta$  diminishes and the states become strongly bound, the energy gap between the even and odd member of the pair vanishes exponentially fast. In fact, one can see in Fig. 2 that the second bound state energy approaches to the first one, the fourth bound state energy approaches to the third one, and so on. In Fig. 3 (a, b) the first even-even and the second odd-even bound states are shown. One can see that we have typical quantum mechanical task of double well potential [31] in which an energy distance between the first and second energy levels becomes exponentially small with growth of a potential barrier between wells. Fig. 3 (c,d) demonstrates the next pair of the bound states in the scissor structure.

Usually the bound state transforms into the quasi-bound state which displays as resonant dip or peak for transmission through the structure as it was observed,

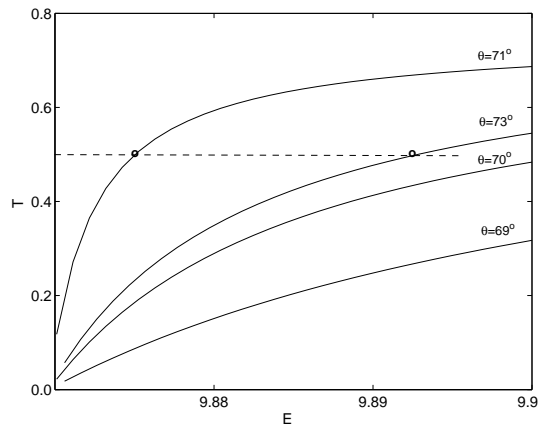


FIG. 4: The probability of transmission through the scissors structure as function of  $E = \lambda k^2$ , eigen value of the Helmholtz equation (11). The transmission probability limits to zero for  $E \rightarrow E_0 = \pi^2$ . Circles show for which  $E$  the transmission probability equals the half.

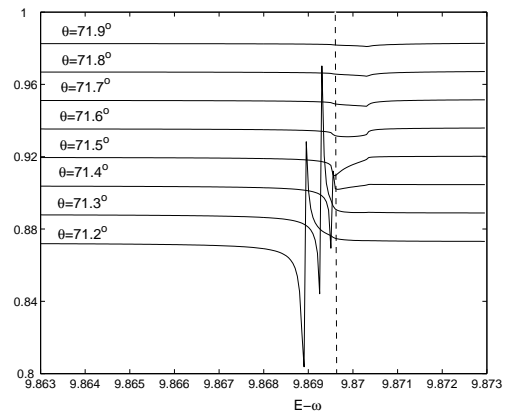


FIG. 5: Evolution of resonant features for the transmission through the scissor structure caused by mixing the propagation state with the bound state via the time-periodic perturbation (21) as the angle of the scissor  $\theta$  increases. The evolution exactly follows to a blow up shown in inset of Fig. 2 for  $\theta \rightarrow \theta_c = 0$ . For the angle exceeding  $\theta_c$  resonant feature is decayed. Dashed vertical line shows the edge of the propagation band  $E_0 = \pi^2$ .

for example, in [30]. However as one can see from Fig. 4 numerical computation of the transmission through the scissor's structure does not show any resonant features for  $\theta > \theta_c \approx 71.5^\circ$ . Also we used the time-periodic perturbation method to search the quasi bound state above  $\theta_c$ . The results of computation in the vicinity of critical angle  $\theta_c$  are shown in Fig. 5.

One can see that for  $\theta < \theta_c$  we have resonant features caused by mixing of propagating mode with the bound state of the time-periodic perturbation. However for  $\theta > \theta_c$  these resonant features do not evolve but only decay with increasing of the angle  $\theta$ . The small wiggle around the value 9.8704 is an artefact of the computation which diminishes with the decrease of  $V_0$ .

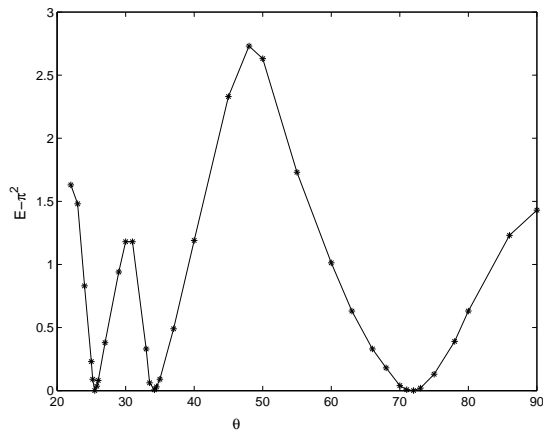


FIG. 6: Distances to the bottom of propagation band at which the transmission takes the half (see Fig. 4) versus the angle of the scissors waveguide.

Moreover for  $\theta$  approaching  $\theta_c$  the transmission probability  $T(E)$  undergoes the following feature as shown in Fig. 4. The less a value  $|\theta - \theta_c|$  the more a slope of the transmission versus  $E$  in the vicinity of  $E - \pi^2$ . For  $\theta \rightarrow \theta_c$  the derivative  $dT/dE \rightarrow \infty$ . If to plot  $E - \pi^2$  at which the transmission is reaching half as shown by circles in Fig. 4 versus the angle of scissor waveguide we obtain remarkable curve shown in Fig. 6. We see that a value  $E - \pi^2$  equals zero just at the critical angles.

### Acknowledgments

This work has been partially by RFBR Grant 01-02-16077, GrantA1048101 of the GAS (P.Exner) and the Royal Swedish Academy of Sciences (A.Sadreev).

\* e-mails: exner@ujf.cas.cz, almsa@ifm.liu.se

- 
- [1] F. Ursell, Proc. Roy. Soc. **47**, 79 (1952)
- [2] M.L. Roukes, A. Scherer, S.J. Allen, Jr., H.G. Craighead, R.M. Ruthen, E.D. Beebe, and J.P. Harbison, Phys. Rev. Lett. **59**, 3011 (1987)
- [3] G. Timp, H.U. Baranger, P. de Vegvar, J.E. Cunningham, R.E. Howard, R. Behringer, and M.M. Mankiewich, Phys. Rev. Lett. **60**, 2081 (1988)
- [4] P. Exner and P. Šeba, J. Math. Phys. **30**, 2574 (1989)
- [5] P. Exner, P. Šeba, and P. Štoviček, Czech. J. Phys. **B39**, 1181 (1989)
- [6] P. Exner, Phys. Lett. **A141**, 213 (1989)
- [7] R.L. Schult, D.G. Ravenhall, and H.W. Wyld, Phys. Rev. **B39** 5476 (1989)
- [8] F.M. Peeters, Superlatt. Microstruct. **6**, 217 (1989)
- [9] P. Exner and P. Šeba, Phys. Lett. **A144**, 347 (1990)
- [10] Y. Avishai, D. Bessis, B.G. Giraud, and G. Mantica, Phys. Rev. **B44**, 8028 (1992)
- [11] J. Goldstone and R.L. Jaffe, Phys. Rev. **B45**, 14100 (1992)
- [12] J.P. Carini, J.T. Londergan, K. Mullen, and D.P. Murdock, Phys. Rev. **B46**, 15538 (1992)
- [13] J.P. Carini, J.T. Londergan, K. Mullen, and D.P. Murdock, Phys. Rev. **B48**, 4503 (1993)
- [14] J.P. Carini, J.T. Londergan, D.P. Murdock, D. Trinkle, C.S. Yung, Phys. Rev. **B55**, 9842 (1997)
- [15] E.N. Bulgakov and A.F. Sadreev, JETP Letters, **66**, 431 (1997)
- [16] E.N. Bulgakov and A.F. Sadreev, Technical Phys. **46**, 1281 (2001)
- [17] J.T. Londergan, J.P. Carini, D.P. Murdock: *Binding and Scattering in Two-Dimensional Systems. Applications to Quantum Wires, Waveguides and Photonic Crystals*, Springer LNP m60, Berlin 1999
- [18] E.N. Bulgakov and A.F. Sadreev, Europhys. Lett. **57**, 198 (2002).
- [19] B. Lax, K.J. Button, *Microwave Ferrites and Ferrimagnetics*, N.Y., 1962.
- [20] M. Reed and B. Simon: *Methods of Modern Mathematical Physics, IV. Analysis of Operators*, Academic Press, New York 1978; Sec. XIII.15.
- [21] T. Kato: *Perturbation Theory for Linear Operators*, 2nd edition, Springer, Berlin 1976; Sec. VIII.6.
- [22] F. Bentosela, P. Exner, V.A. Zagrebnov, Phys. Rev. B **57**, 1382 (1998)
- [23] R.J.Riddell, Jr, J. Comp. Phys. **31**, 21, 42 (1979)
- [24] J. Aguilar and J.-M. Combes, Commun. Math. Phys. **22**, 269 (1971)
- [25] N. Moiseyev, Phys. Rep. **20**, 211 (1998)
- [26] P. Duclos, P. Exner, P. Štoviček, Ann. Inst. H. Poincaré: Phys. Théor. **62**, 81 (1995)
- [27] P. Šeba, I. Rotter, M. Muller, E. Persson, K. Pichugin, Phys. Rev. **E61**, 66 (2000)
- [28] E.N. Bulgakov and A.F. Sadreev, JETP **87**, 1058 (1998)
- [29] G. Burmeister and K. Maschke, Phys. Rev. **B59**, 4612 (1999).
- [30] P. Exner and D. Krejčířik, J. Phys. A **32**, 4475 (1999)
- [31] L.D. Landau and E.M. Lifshitz, *Quantum Mechanics*, Pergamon Press, N.Y., 1965